KYOTO UNIVERSITY

NRE Discussion Papers No. 2025-03
May 2025
Division of Natural Resource Economics, Graduate School of Agriculture, Kyoto University

How rational are individuals in asset price formation?
Impact assessment of the 2018 Taiwan flood and land subsidence on farmland prices

Yu-Ching Shen and Kei Kajisa

May 8, 2025

Discussion Papers Natural Resource Economics Discussion Papers are preliminary research reports by members of the GSA-NRE Kyoto University circulated for comments and suggestions. They have not been externally peer-reviewed or been subject to the review by the editorial board. All rights are reserved by the authors.

Faculty/Graduate School of AGRICULTURE KYOTO UNIVERSITY

Division of Natural Resource Economics
Kitashirakawa Oiwake-cho, Sakyo-ku, Kyoto 606-8502, Japan

How rational are individuals in asset price formation? Impact assessment of the 2018 Taiwan flood and land subsidence on farmland prices

Yu-Ching Shen and Kei Kajisa

Abstract

This study examined whether and how actual floods affect farmland price formation, using the case of the severe flood that occurred in August 2018 in Taiwan. We used two newly constructed datasets: one constructed from Synthetic Aperture Radar imagery to capture flood exposure and the other based on contour maps to measure land subsidence (LS). Applying the triple difference method, we found that farmland prices in flood-affected areas were already 13.4% lower than those in flood-free areas prior to the flood at the village level. Furthermore, we found no statistically significant effect of the actual flood on farmland prices at conventional levels of significance. We argue that the farmland prices were sufficiently low even before the flood and, thus, was not adjusted after the flood, implying people rationally formed farmland price. Our results also indicate that every 1-meter of subsidence reduced farmland prices per square meter by 14.2%. However, unlike the case of flood, the low ex-ante price of subsided land became even lower after the actual flood. This implies that the LS, as a relatively new and unfamiliar event, cannot be fully incorporated in the price formation. Our findings suggest that while familiar and historically observed risks, such as flooding, are appropriately incorporated into farmland valuations, newer risks like land subsidence may not be. This underscores the importance of frequently updating hazard maps in response to evolving environmental risks, so that individuals can make informed decisions based on the most current information available.

Keywords: Asset price formation, Farmland price, Flood risk, Land subsidence, Rational expectations

1. Introduction

Due to climate change, the frequency and scale of extreme weather events are increasing. Heavy rainfall in many places worldwide has caused floods and, therefore, significant damages. Under these circumstances, the risk to properties such as land and houses is increasing. Over 3,800 major flood events were reported from 2001 to 2023, which had resulted in economic losses of over 820 billion USD globally (CRED, 2021; CRED, 2022; CRED, 2023). Floods not only create current and future

losses but also increase uncertainty of future revenues, significantly reducing the expected current land value. To ensure a well-functioning market and efficient resource allocation, the changes in flood risks and the corresponding changes in property value should be fully reflected in property price.

Most past studies used hazard maps to assess the impact of flood risk on property prices (Atreya et al., 2013; Beltrán et al., 2018; Bin and Landry, 2013; Koks et al., 2015; Fletcher et al., 2022; Ortega and Taspinar, 2018). A hazard map is a graphical information medium indicating the severeness of possible floods in the future. Some studies used ex-ante hazard information to assess the impact of an actual flood event, while others relied on ex-post hazard information which was updated by the actual flood whose impact they wanted to estimate. Regardless of the measurement's timing, existing studies used hazard maps as a proxy for the actual floods; thus, the impact estimated was the impact of *potential* floods, rather than the impact of actual floods. Most studies identified a negative impact of potential flood risk on property prices.

Meanwhile, some studies show that such a negative price updating is characterized by unawareness, myopic thinking, and poor recollection, resulting in the incomplete updating of flood risk (Fletcher et al., 2022). Another group of studies shows that the effect on price is short-lived and, thus, the price returns even to the original level in the long run (Atreya et al., 2013; Bin and Landry, 2013; Fletcher et al., 2022). These price changes could be considered as re-adjustment toward the true land price.

However, it has not been examined yet whether the updating and re-adjusting of property price fully and accurately reflect the changes in true property value because empirical studies examining the impact of the *actual* flood are scarce. If property prices fully incorporate the flood risk with an updated hazard map information together with the local knowledge accumulated through past experiences, prices should not significantly change after the actual flood, indicating a rational price formation.

Few studies used the actual inundation of properties to capture the severeness of actual floods. These studies used house prices and, thus, may ignore the impact of minor floods because houses would not be damaged. (Daniel et al., 2009; Beltrán et al., 2019). Therefore, the impact evaluation of land, which can be more susceptible to minor floods, is missing. Moreover, the geospatial simulation-based identification of inundated areas used by the existing studies could still have measurement inaccuracies as they are not actual observations (Atreya and Ferreira, 2015). To better understand whether people rationally set property prices by fully and accurately accounting for risks, we must examine the impact of the actual flood on land prices.

This study examines whether and how an actual flood affects farmland prices,

using the case of the severe flood that occurred in August 2018 in Taiwan. To answer this question, we utilize two newly constructed datasets developed by the authors: the indicator of actual flood experience, derived from the synthetic aperture radar (SAR) image analysis, and the level of accumulative land subsidence (LS), measured by means of the LS maps made by Water Resource Agency from the 1990s until the time the farmland is transacted. The SAR image analysis can generate accurate and granular plot-level images of flooded areas. The level of accumulative LS can capture the influence of the relatively new and unknown events that can increase flood risk. Our analysis focuses on farmland prices because LS mostly occurred on farmland.

We applied the triple difference method to our data and found that the farmland price had been sufficiently low even before the flood and, thus, was not adjusted after the flood, indicating people rationally formed farmland price. Simultaneously, the impact of LS, which was a relatively new and unforeseeable event for farmers to perceive its potential impact with strong rainfall, cannot be fully incorporated into the price and, thus, the low ex-ante price in the flood-affected areas became even lower after the actual flood experience in the subsided lands. This suggests that updating information (e.g., information on LS level and associated risks) and obtaining it from reliable sources is important.

The remainder of this paper is structured as follows. Section 2 introduces the background of the study site and the flood we utilize. Section 3 explains our main dataset. Section 4 provides our empirical strategy and the econometric model specification. Section 5 presents our estimation results and discusses the price formation mechanism based on our findings. Finally, Section 6 provides the conclusion.

2. Background of study site and the August 2018 flood in Taiwan

2.1 Study site

Taiwan is prone to massive storms, tropical depressions, and strong typhoons between June and September. These weather events cause significant rain, which serves as a crucial source of water for the following six months until next summer. However, the frequency of intense storms has increased due to recent climate changes. Consequently, rainfall intensity increases, but its distribution is more concentrated over several months. Therefore, the floodplain in Taiwan is fertile but prone to floods. Our study site is on this flood plain in central and southern Taiwan and takes advantage of fertility but faces the risk of flooding.

The study site comprises Changhua County, Yunlin County, Chiayi County, Chiayi City, and Tainan City (Figure 1). These five cities specialized in producing rice and vegetables, producing almost a half of Taiwan’s agricultural product values.

Due to the 2018 disaster, over 40% of the agricultural crop losses in Taiwan occurred in these areas (Ministry of Agriculture, 2018). These five cities and counties accounted for 39% of Taiwan's farmland area, 45% of the country's agricultural production value, 63% of animal husbandry production value, and 25% of fishery production value in 2023, as shown in Table 1. While they are regarded as the granary of Taiwan, they also bear significant costs. Groundwater exploitation remains a critical issue in these cities because the subsiding area in these five cities reached 688 km^2 by 2021 (LSPRC, 2022).

2.2 August 2018 flood in Taiwan

This study uses a flood event in central and southern Taiwan as a treatment to the farmland. The flood analyzed in this study continued from August 23 to 28 in 2018, resulting in losses of 31.5 million dollar for the agricultural sector. The two most severely affected areas, Chiayi County and Tainan City, accounted for 53% and 25% of total losses, respectively. Additionally, seven people were killed, two people went missing, and around 150 people got injured, while 2,042 people needed to evacuate to 77 shelters. Many places, such as Yunlin, Chiayi, and Tainan, had recorded over 500 millimeters of rainfall in 24 hours on August 23, 24, and 28. Some places even recorded over 100 mm of rain in one hour.

3. Data

3.1 Farmland transaction data

Following related past studies, we adopt transacted property prices as our main outcome variable. This study uses the dataset of farmland transaction records from the Actual Price Registration System (APRS), which was developed by the Ministry of the Interior in Taiwan in August 2012. With this system, reporting every real estate-related transaction is mandatory. The sales price, transaction date, location data in the format of geographical coordinates, and other transaction characteristics such as its zoning, building specification, and usage are collected. The APRS dataset is the most detailed information source on the real estate market in Taiwan. We restricted the analytical sample to farmlands because, as explained in the introduction, LS occurs mostly on farmlands. Although we found that the same plots were transacted multiple times during the period covered by our dataset (January 2016 to July 2020), we treat our dataset as pooled cross section data rather than unbalanced panel data because the number of such plots is few. The sample size for our analysis is 55,129 and the transaction records by month is shown in Appendix Table A1.

The use of transacted farmland price data may lead to potential selection bias by excluding unobserved prices of non-transacted farmlands. To examine this possibility,

we conduct a *t*-test for the township-level farmland transaction density differences between flooded and flood-free areas. The results in Table 2 show no significant difference in terms of transaction intensity between flooded and flood-free areas, indicating transactions are not concentrated in particular areas in terms of flood experience. Additionally, we compute a correlation coefficient between the level of LS and the farmland transaction density in the area of each LS level. The results in Table 3 show no significant tendency along the level of LS, again indicating that transactions are not concentrated in particular areas in terms of LS.

3.2 Synthetic Aperture Radar (SAR) images

SAR images are used for geographical analysis to distinguish the water, paddy, ground, and buildings as those objects in the SAR images are categorized by the reflection rate of their surface and simplified as light or dark area. We conducted flood mapping through Google Earth Engine, which allowed us to access preprocessed SAR imagery. The raw imageries of Sentinel-1 were preprocessed to filter the data down to a homogeneous subset. Steps such as Ground Range Detected (GRD) border and thermal noise removal, as well as terrain correction, were performed by Google Earth Engine to ensure consistent analysis.

Following Chiu et al. (2019), this study identified the inundated area as follows (Figure 2). First, we collected two SAR Satellite images: before (2018/08/20) and after (2018/08/26) the flood from the Sentinel-1 satellite developed by the European Space Agency (ESA). The SAR map indicates open water in black color. Hence, comparing two images of study sites before and after the flood, we judged that the areas newly indicated in black color were new open water bodies resulting from the flood. The blue areas in the right figure in Figure 2 indicate new black areas after the flood. The inundated area we detected is shown in Figure 3, which is used as the indicator of the flood affected areas in this paper.

3.3 Land Subsidence (LS)

Overusing groundwater is the primary source of LS in Taiwan. Groundwater in Taiwan has two main uses: agricultural activities and residential consumption. Many agricultural activities, such as irrigation and aquaculture, prefer using groundwater since it is low in temperature in summer, cheap, and stable. Conversely, regarding urban residential consumption, such as tap water supply, cities located in plains without any reservoirs (e.g., Yunlin and a part of Changhua) must rely on the groundwater.

The LS maps, prepared by the National Science and Technology Center for Disaster Reduction, Taiwan, provide information to understand the magnitude of LS

in the study regions. The earliest records of LS in Taiwan can be traced back to the 1990s, with contour maps being collected annually. We generated the plot level LS data from the map of the year when that plot was transacted. For example, if the land was transacted in 2016, the LS was collected on the location in the map in 2016 which indicates the accumulative subsidence since 1990.

Figure 4 illustrates the accumulative LS amount from 1990 to 2016, 2017, 2018, 2019, and 2020, respectively, indicating greater LS areas with darker orange. Two severely subsided areas (Changhua and Chiayi) are close to the coastline since aquaculture and paddy irrigation intensively use groundwater. Problems caused by LS are soil salinization and seawater intrusion because seawater occupies the area after groundwater extraction. Furthermore, the land subsided unevenly since the support provided by the groundwater layer vanished unevenly. Moreover, the lower elevation of subsidence areas aggravates the risk of flooding.

3.4 Variables' definitions and descriptive statistics

The core idea of the hedonic pricing model (HPM) suggests that a consumer's utility depends on the characteristics of a good or service consumed (Rosen, 1974). This perspective is frequently applied to land lots. As for farmland, farmland prices are linked to disaster-related, agricultural, and non-agricultural characteristics. Table 4 presents the list of dependent and explanatory variables, their definitions, and the descriptive statistics. Our dependent variable is farmland price per m^2 deflated by the consumer price index in 2016 (1,000 USD/m^2). Key variables for impact assessment include a dummy variable which takes the value of one if farmland is detected in the inundated area by the SAR imagery analysis (treatment dummy), a dummy taking the value of one after the flood of August 23rd in 2018, and the level of accumulative land subsidence from 1990 till the land transaction (m). As agricultural characteristics, we used land size (1,000 m^2), land productivity measured by soil pH, and soil water retention index ranging from 1 to 3 (higher the index, the higher the retention capacity). As non-agricultural characteristics, we employed four types of the nearest distance variables from the farmland (km): agricultural association, highway, province road, and the Taiwan High Speed Rail station.

Figure 5 shows the trend of the monthly average farmland prices by flood experience during our sample period (from January 2016 to July 2020). We found that the price level of farmlands that experienced the August 2018 flood (blue line) is lower than farmlands that did not experience it (orange line). Furthermore, they shared a similar price fluctuation pattern before the event (left of the dashed vertical line).

4. Methodology

4.1 The event study analysis

Difference-in-difference (DID) design is one of the most powerful causal inference econometric models. The impact of interest on the outcome variable is measured by the difference between two values. One is the difference of the outcome variable between treatment and control groups before the event, while the other is the same difference after the event. To make a valid comparison, these two groups must meet the common trend assumption.

Therefore, we conduct the event study analysis using the following model.

$$ln(Price_{ijkt}) = \beta_0 + \sum_{t=-31}^{-1} \alpha_t \, Pre_t + \sum_{t=1}^{23} \alpha_t \, Post_t + \beta_1 Flood_{ijk} + \sum_{t=-31}^{-1} \gamma_t \left(Pre_t \times Flood_{ijk}\right) + \sum_{t=1}^{23} \gamma_t \left(Post_t \times Flood_{ijk}\right) + \boldsymbol{X_{ijkt}\delta} + \tau_{jt} + \varepsilon_{ijk} \quad (1)$$

where $ln(Price_{ijkt})$ is the log of observed farmland transaction price of farmland *i* located in village *j* of the township *k* in farmland transaction period (month-year) *t*. Pre_t and $Post_t$ are dummy variables referring to each month from January 2016 to July 2020 except for the benchmark month, August 2018. There are 31 pre-period and 23 post-period dummy variables in total. Those dummy variables equal one if farmland *i* was transacted in period *t*; $Flood_{ijk}$ is a treatment dummy taking the value of one if farmland *i* in village *j* of the township *k* is identified as inundated due to the flood in 2018 by the SAR satellite images. $\boldsymbol{X_{ijkt}}$ is a set of explanatory variables shown in Table 4. β_0, $\beta_1, \alpha_t \, \gamma_t$, and $\boldsymbol{\delta}$ are parameters to be estimated, while ε_{ijkt} is the error term. A fixed effect term τ_{jt} in Equation (1) captures the month*village fixed effect. The coefficients γ_t show the impact of flood on farmland price at each month.

Figure 6 shows the results of the event study analysis based on Equation (1). The vertical dot line indicates the benchmark month, when the flood occurred. No coefficients significantly differ from zero before the event, indicating that the treatment and control groups meet the common trend assumption. Even after the event, the figure shows no significant coefficients statistically different from zero. This implies that farmland price was not affected by the flood. To investigate this aspect with more statistical rigor, we apply a triple difference design, which also allows us to examine whether the impact of the flood shows a heterogeneous pattern between the LS and LS-free areas.

4.2 Triple Difference design

We set our triple DID as follows.

$$\begin{aligned} ln(Price_{ijkt}) = {} & \beta_0 + \alpha_1 After_t + \beta_1 Flood_{ijk} + \gamma_1 After_t \times Flood_{ijk} \\ & + \varphi_1 Landsub_{ijkt} + \alpha_2 Landsub_{ijkt} \times After_t \\ & + \beta_2 Landsub_{ijkt} \times Flood_{ijk} + \gamma_2 Landsub_{ijkt} \times After_t \times Flood_{ijk} \\ & + \boldsymbol{X_{ijkt}\delta} + \tau_{jt} + \varepsilon_{ijk} \qquad (2) \end{aligned}$$

where we have two new variables: $Landsub_{ijkt}$ is the level of accumulative LS and $After_t$ is a dummy variable equal to one after August 2018. Standard errors are clustered at the village level, the lower level next to the township in the administrative district system. The triple difference term ($Landsub_{ijkt} \times After_t \times Flood_{ijk}$) captures how much the price of subsided farmland decreased after the flood. The fixed effect term τ_{jt} in Equation (2) captures the month*village fixed effects. As an alternative model, we use τ_{kt} to replace τ_{jt} by controlling for the month*township fixed effects. This is because *Landsub* and *ln(Price)* have few within-village variations; thus, the month*village fixed effects capture most of the variations. For example, the result of one-way ANOVA for dependent variable *ln(Price)* in Table 5 indicates that the mean square of *ln(Price)* within-village (0.43) is by far smaller than that of between-village (36.22). One-way ANOVA for LS in Table 5 shows a similar pattern to that of *ln(Price)*. Hence, the impact appears homogenous within-village. Differential impacts seem to arise between villages or in geographically larger areas, and to capture them, we use the model with month*township fixed effects.

5. Results and Discussion

Table 6 shows the estimation results.[1] The results indicate that farmland prices in the treatment group are significantly lower than those in the control group when controlling for month-by-township fixed effects in Column (2), indicating that prices of farmland located in the flood-affected areas are lower than those in the flood-free areas by 13.4%. Meanwhile, the difference in farmland prices between the treatment and control groups becomes statistically insignificant when controlling for month-by-village fixed effects in Column (1). This difference stems from the fact that variations generated between villages, not within a village, which we examined through ANOVA analyses in Table 5. The coefficients of the DID estimator, *After* * *Flood*, are insignificant at any conventional level in both columns. We argue that the

[1] The complete results are shown in Appendix Table A2.

farmland price was sufficiently low even before the flood and, thus, was not adjusted after the flood, implying that people rationally formed farmland price expectations.

The coefficient of LS is negative and statistically significant in Column (2). The results indicate that every 1-meter of subsidence reduces farmland prices per square meter by 14.2% at the village level. The triple difference term (*LS*After*Flood*) has a negative and significant coefficient in Column (2). Combining these results, we infer that people regard LS as an environmental disamenity and consider the LS information in their farmland price formation. However, whether LS exacerbates the flood risk of farmland or not must have remained unclear to people. Therefore, the impact of LS must not have been fully incorporated into the price formation and, thus, the low ex-ante farmland price in flood-affected areas further decreased after the actual flood in subsided lands. These findings suggest that updating information (e.g., information on LS level and associated risks) and obtaining it from a reliable source is important.

6. Conclusion

This study examined how farmland market had taken flood risk into account in its price formation, using the great flood in Taiwan in August 2018. We found that the flooded area's farmland price was lower before the flood and no adjustment occurred after the event. Our findings imply that people rationally incorporate the risks into farmland price if they are familiar with that event. However, this does not hold for relatively new events such as land subsidence. This suggests that a hazard map should be renewed as frequently as the risks change, so that people update their knowledge on the unfamiliar risks and have clearer knowledge of the potential flood-affected areas.

This study has some limitations. First, the data of APRS are provided by the government for public use; therefore, the related personal information of buyers and sellers are not accessible. Second, due to the limited numbers of multiple transactions of the same farmlands, we cannot construct balanced panel data to control for spatial heterogeneity by using spatial weighted matrix. Future studies should compare the impact assessment of floods on non-farm land assets such as residential land and housing.

Acknowledgments

We thank Ken Miura and Yohei Mitani for their valuable comments. Shen would like to acknowledge a scholarship by LOTTE Foundation for his graduate study.

References

Atreya, A., Ferreira, S., Kriesel, W., 2013. Forgetting the flood? An analysis of the flood risk discount over time. Land Economics. 89(4), 577–596.

Atreya, A., Ferreira, S., 2015. Seeing is believing? Evidence from property prices in inundated areas. Risk Analysis. 35(5), 828-848.

Beltrán, A., Maddison, D., Elliott, R. J R., 2018. Is Flood Risk Capitalised Into Property Values?. Ecological Economics. 146, 668–685.

Beltrán, A., Maddison, D., Elliott, R. J R., 2019. The impact of flooding on property prices: A repeat-sales approach. Journal of Environmental Economics and Management. 95, 62–86.

Bin, O., Landry, C.E., 2013 Changes in implicit flood risk premiums: empirical evidence from the housing market. Journal of Environmental Economics and Management. 65 (3), 361–376.

Centre for Research on the Epidemiology of Disasters (CRED), 2023. The annual report of Emergency Events Database EM-DAT. https://files.emdat.be/reports/2023_EMDAT_report.pdf (accessed 18 December 2024).

Centre for Research on the Epidemiology of Disasters (CRED), 2022. The annual report of Emergency Events Database EM-DAT. https://www.cred.be/sites/default/files/2022_EMDAT_report.pdf (accessed 18 December 2024).

Centre for Research on the Epidemiology of Disasters (CRED), 2021. The annual report of Emergency Events Database EM-DAT. https://www.cred.be/sites/default/files/2021_EMDAT_report.pdf (accessed 18 December 2024).

Chiu, C. Y., Hsieh, C. S., Huang, T. J., Yeh, K. S., Kuan, L. H., Hu, J. C., 2019. A Study for Inundation Mapping After Typhoon and Heavy Rainfall by Using SAR Imagery. Journal of Photogrammetry and Remote Sensing. 24(4), 211-222.

Council of Agriculture, Executive Yuan, 2018. The Report of the structure and index of Agricultural sector production value. https://agrstat.coa.gov.tw/sdweb/public/inquiry/InquireAdvance.aspx (accessed 26

September 2020).

Daniel, V. E., Florax, R. J., Rietveld, P., 2009. Floods and residential property values: a hedonic price analysis for The Netherlands. Built Environment. 35(4), 563-576.

Fletcher, C. S., Ganegodage, K. R., Hildenbrand, M. D., Rambaldi, A. N., 2022. The behaviour of property prices when affected by infrequent floods. Land Use Policy. 122, 106378.

Koks, E.E., Jongman, B., Husby, T.G., Botzen, W.J.W., 2015. Combining hazard, exposure and social vulnerability to provide lessons for flood risk management. Environmental Science Policy. 47, 42-52.

LSPRC, 2022. Information for Prevention and Monitoring of Land Subsidence in Taiwan, Cheng Kung University (LSPRC). http://www.lsprc.ncku.edu.tw/zh-tw/trend.php?action=view&id=4 (accessed 30 January 2022).

Rosen, S., 1974. Hedonic Prices and Implicit Markets: Product Differentiation in Pure Competition. Journal of Political Economy. 82(1), 34–55.

Ortega, F., Taspinar, S., 2018. Rising sea levels and sinking property values: Hurricane sandy and New York's housing market. Journal of Urban Economics. 106, 81–100.

Table 1. The characteristics of study sites in 2023

	Taiwan	Study sites' total	Changhua County	Yunlin County	Chiayi County	Chiayi City	Tainan City
Farmland Area (1,000 ha)	77.9	39%	8%	10%	9%	0.2%	12%
Production value of agriculture (1,000 thousand NTD)	275.3	45%	10%	15%	9%	0.2%	11%
Production value of animal husbandry (1,000 thousand NTD)	214.9	63%	20%	21%	9%	0.1%	13%
Production value of fish product (1,000 thousand NTD)	90.5	25%	2%	7%	7%	0.0%	9%

Data Source: Ministry of Agriculture, R.O.C (Taiwan)

Table 2. *T*-test result of the farmland transaction density differences between flooded and flood-free areas in townships

Variable	Number of observations	Mean	Std. Err	Std. Dev
Density difference	100	-0.33	0.55	5.51
H_0: mean = 0	t = -0.60	*p-value* = 0.55		

Note: There are 55,129 farmland transactions across 100 townships. The transaction density for flooded and flood-free areas in each township is calculated, which yields 100 paired observations of transaction densities. A *t*-test is applied to the differences of the pairs to examine whether the occurrence of transactions statistically differs from zero between flooded and flood-free areas in townships.

Table 3. Correlation coefficient between the level of LS and the farmland transaction density at each LS level

Variable	LS level from 0 to 210	Density in the area of each LS level from 0 to 210
LS level from 0 to 210	1.000	
Density in the area of each LS level from 0 to 210	0.177 (0.377)	1.000

Note: *p*-value for statistical significance of correlation coefficient is in parentheses. There are 55,129 farmland transactions. The transaction density is calculated at each level of LS (27 levels from 0 cm to 210 cm), which yields 27 observations of transaction densities. The correlation coefficient between the levels of LS and the farmland transaction densities at each LS level is calculated along with its statistical significance.

Table 4. Definition and descriptive statistics of dependent and explanatory variables

		Level of variations	Mean	Std.Dev.	Min.	Max.
Dependent Variable						
Price	Farmland price deflated by the consumer price index, using year 2016 as the base year ($1,000USD / m^2)	Plot *i* Time *t*	0.10	0.11	0.00	0.60
Disaster-related Variable						
Flood (treatment)	=1 if farmlands are detected as the inundated area after Aug.23 2018; otherwise, = 0.	Plot *i* only	0.03	0.18	0.00	1.00
After	=1 if farmland transaction happened after Aug. 23, 2018; otherwise, = 0.	Time *t* only	0.43	0.49	0.00	1.00
Land Subsidence (LS)	The level of accumulative subsidence from 1990 to the year transaction occurred (m)	Plot *i* only	0.32	0.43	0.00	2.10
Agricultural Characteristics						
Land Size	Transacted farmland size (1,000 m^2)	Plot *i* only	2.38	10.24	0.00	1411.46
Land productivity	Soil pH measurements in H_2O, proxy of productivity.	Plot *i* only	4.92	3.07	0.00	9.41
Soil water retention index	The index measuring the capacity to keep water in soil, From 1 to 3, The higher the value is, the more capable to keep water in soil are.	Plot *i* only	1.22	0.70	0.00	3.00
Non-agricultural Characteristics			3.17	1.63	0.04	16.32
Agricultural Association	Distance to the nearest Agricultural association of each township (km)	Plot *i* only	6.42	6.03	0.00	29.13
Highway	Distance to the nearest highway interchange (km)	Plot *i* only	1.95	1.78	0.00	14.80
Main road	Distance to the nearest province roads (km)	Plot *i* only	9.12	6.42	0.00	46.33
Taiwan High Speed Rail	Distance to the nearest Taiwan High Speed Rail station (km)	Plot *i* only	0.10	0.11	0.00	0.60
No. of observations			55,129			

Data Source: Ministry of the Interior, R.O.C (Taiwan)

Table 5. One-way Analysis of Variance for farmland price and land subsidence

Panel A: *ln(Price)*					
Source	Sum of Squares, SS	Degree of freedom	Mean Square, MS	*F*	*p*-value
Between village	38394.95	1,065	36.05	83.05	0.000
Within village	23468.89	54,063	0.43		
Total	61863.84	55,128	1.12		
Panel B: *Landsub* (LS)					
Source	Sum of Squares, SS	Degree of freedom	Mean Square, MS	*F*	*p*-value
Between village	10065.52	1,065	9.45	1638.03	0.000
Within village	311.94	54,063	0.01		
Total	10377.45	55,128	0.19		

Note: There are 55,129 farmland transactions across 1,066 villages. A one-way analysis of variance (ANOVA) is applied to the dependent variable, *ln(Price)*, and the land subsidence variable, *Landsub*, to examine the extent of variation between and within villages.

Table 6. Triple difference regression results explaining the impact of flood and land subsidence on log farmland price (farm plot level analysis)

	(1) Month and village Fixed effects	(2) Month and Township Fixed effects
Flood (treatment)	-0.0718	-0.1344***
	(0.052)	(0.034)
After * Flood	0.0079	0.0301
	(0.079)	(0.046)
Land Subsidence (LS)	0.0251	-0.1424**
	(0.133)	(0.063)
LS * Flood	-0.0265	-0.0048
	(0.138)	(0.061)
LS * After	0.0224	0.0716
	(0.067)	(0.046)
LS * After * Flood	-0.0575	-0.1073**
	(0.091)	(0.053)
Observations	55,129	55,129
R^2	0.84	0.62
F	19.39	62.88
p-value	0.00	0.00
Fixed Effect	Month*village	Month*Township
Cluster SE	village	village
Control Variables	Yes	Yes

The variable "After" does not appear alone on the table as it has been absorbed by month fixed effects. Standard errors in parentheses. Control variables: *ln(Land Size)*, *Land Productivity*, *Soil water retention index*, *ln(Agricultural Association)*, *ln(Highway)*, *ln(Mainroad)*, and *ln(Taiwan High Speed Rail)*

* $p < 0.10$, ** $p < 0.05$, *** $p < 0.01$;

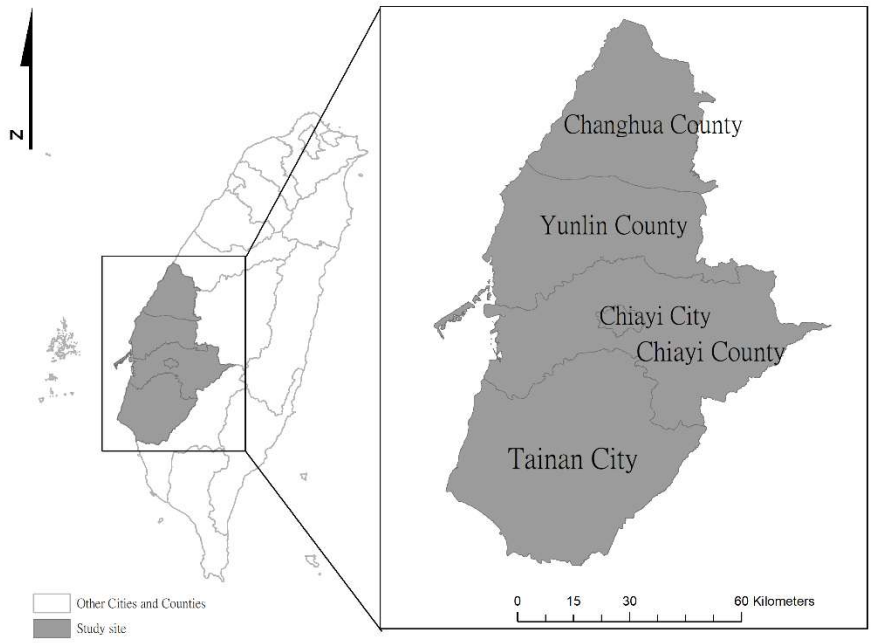


Figure 1. Study sites

Data source: Ministry of the Interior, R.O.C (Taiwan)

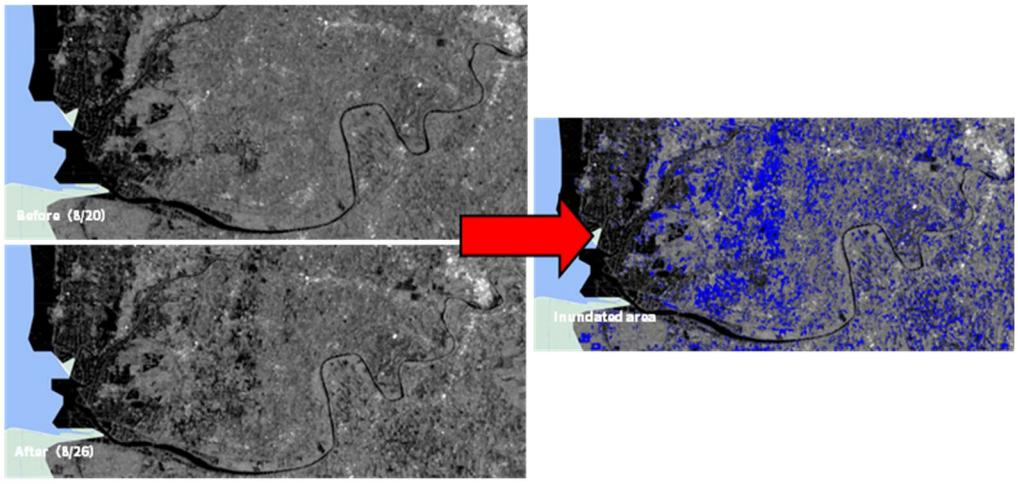


Figure 2. The inundated area identification procedure

Note: The flood occurred after huge rainfall on August 23, 2018. Using two images of study sites before and after flood from Synthetic Aperture Radar (SAR), we detected the new black areas which were new open water bodies resulting from the flood. The blue areas are the new black areas after the flood. The methodology follows Chiu et al. (2019) A Study for Inundation Mapping After Typhoon and Heavy Rainfall by Using SAR Imagery, *Journal of Photogrammetry and Remote Sensing*, 24(4) 211-222.

Data source: European Space Agency (ESA). 2024. Copernicus Sentinel-1 SAR Image Collection. Accessed and analyzed using Google Earth Engine. Available: https://developers.google.com/earth-engine/datasets/catalog/COPERNICUS_S1_GRD.

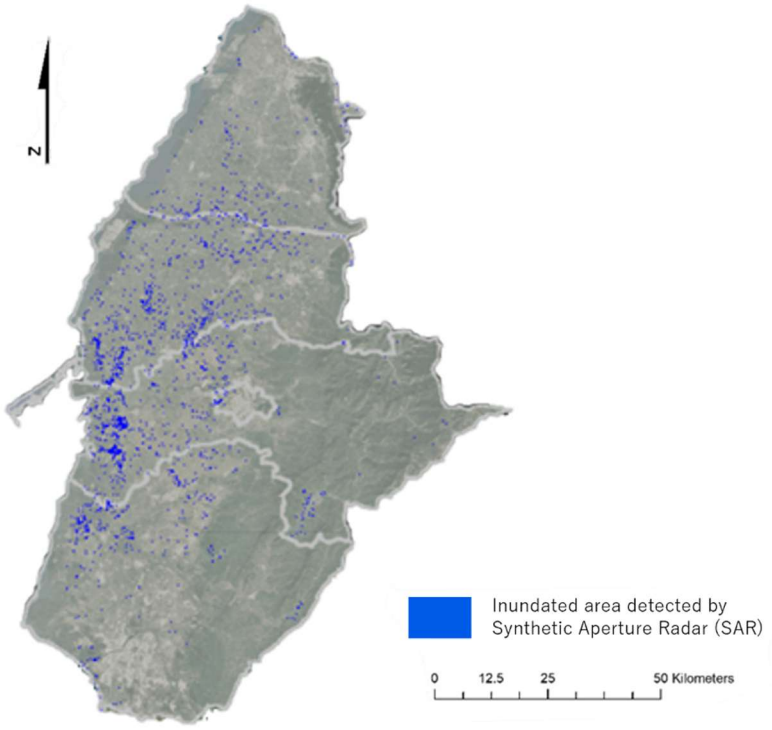


Figure 3. The inundated areas detected by the analysis of Synthetic Aperture Radar (SAR) imagery in the study sites

Note: The dark white line shows the administrative borders between study sites. The blue areas are the inundated areas detected by comparing the change in open water bodies from the Synthetic Aperture Radar (SAR) imagery collected before and after the flood. See the detailed methodology in Figure 2.

Data source: European Space Agency (ESA). 2024. Copernicus Sentinel-1 SAR Image Collection. Accessed and analyzed using Google Earth Engine. Available: https://developers.google.com/earth-engine/datasets/catalog/COPERNICUS_S1_GRD.

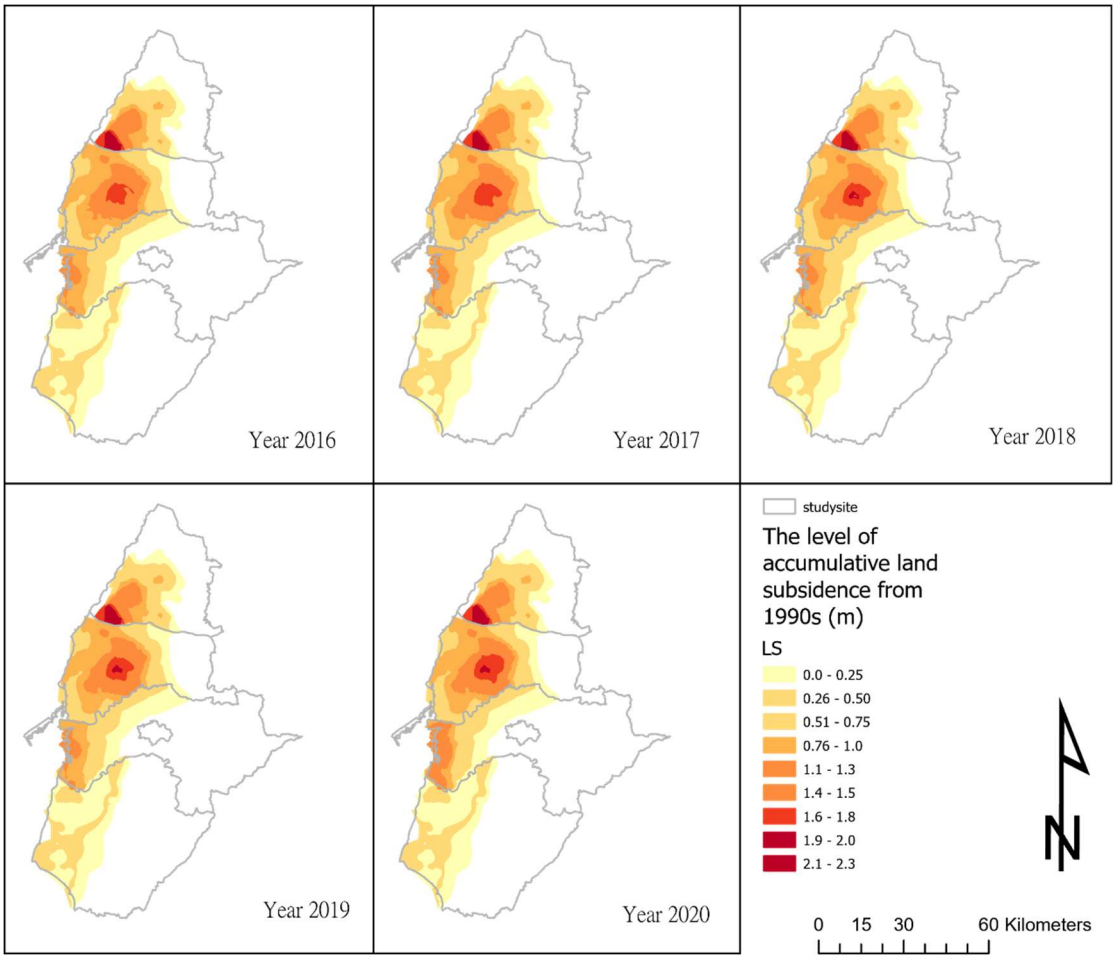


Figure 4. The level of accumulative land subsidence in the study sites from 1990 to the year of measurement (2016, 2017, 2018, 2019, and 2020)

Note: We collected the plot level land subsidence from the map of the year when that plot was transacted. For example, if the land was transacted in 2016, the LS was collected from the location of the map in 2016.

Data Source: Water Resource Agency, Ministry of Economic Affairs, R.O.C (Taiwan)

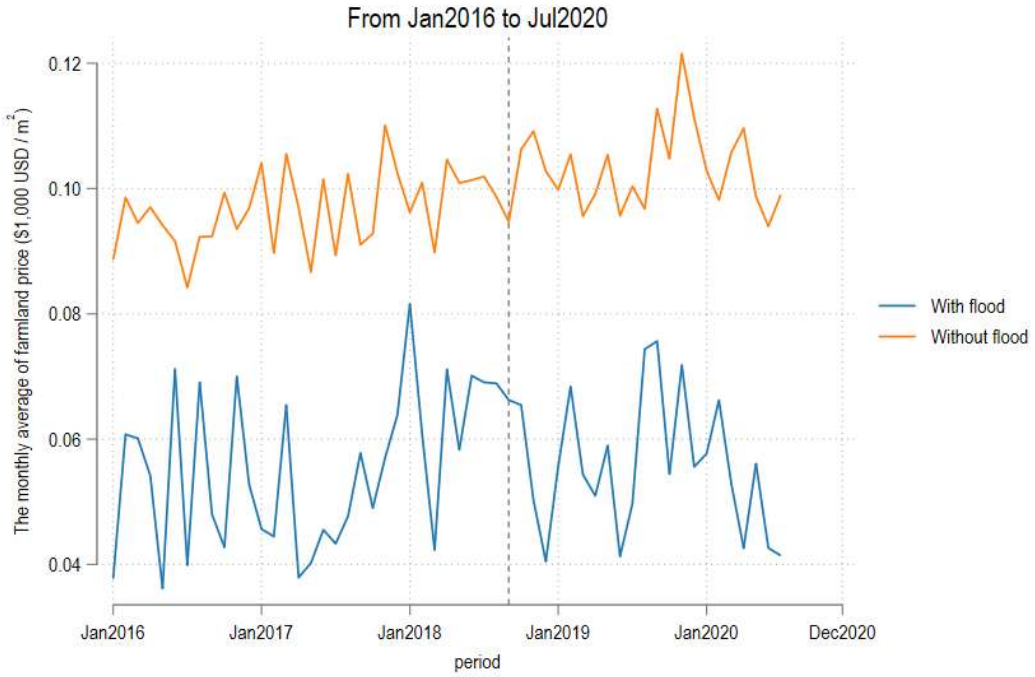


Figure 5. The trend of the monthly average farmland prices by flood experience from Jan. 2016 to Jul. 2020.

Data source: Ministry of the Interior, R.O.C (Taiwan)

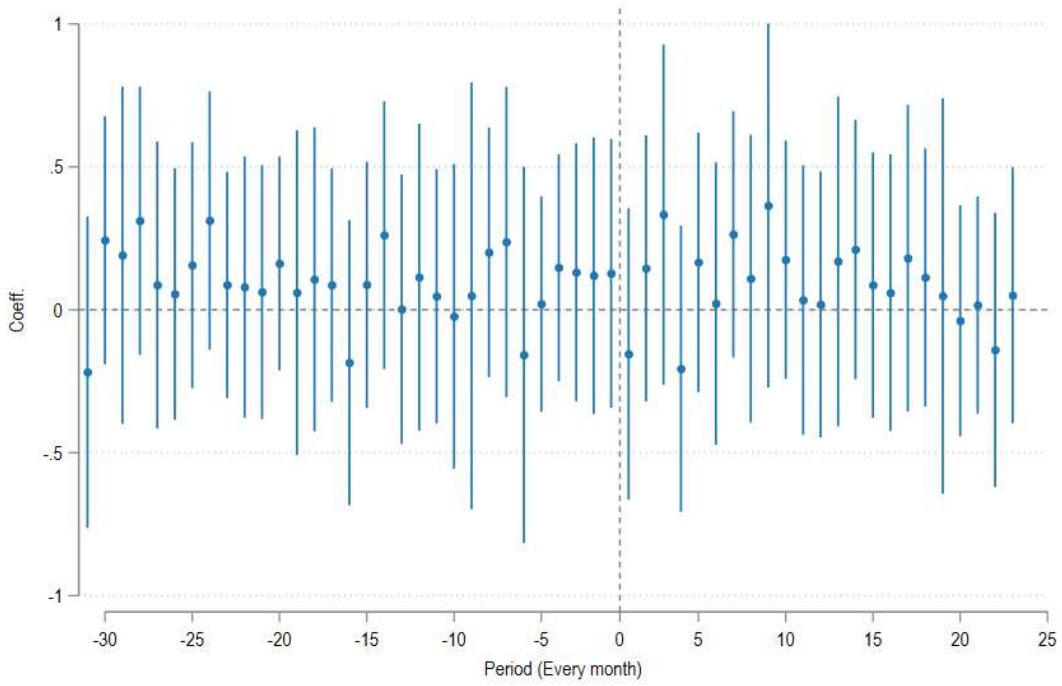


Figure 6. The coefficient plot of log of plot-level farmland price event study comparing with-flood and without-flood plots.

Note: The benchmark month is Aug 2018. The pre-period began from Jan 2016 to Jul 2018, with 31 periods in total. The post-period began from Sep 2018 to July 2020, with 23 periods in total.

Appendix

Table A1. The number of transaction records, by village and township

Month	Number of transaction records	Number of village	Number of township	Average of the number of transactions within a village
Jan-2016	654	388	96	2.4
Feb-2016	522	342	98	2.0
Mar-2016	987	473	98	3.3
Apr-2016	948	473	96	3.0
May-2016	1,004	499	97	3.1
Jun-2016	907	473	97	3.2
Jul-2016	1,028	497	97	4.3
Aug-2016	988	480	97	3.8
Sep-2016	988	449	97	7.8
Oct-2016	939	454	96	5.2
Nov-2016	1,001	487	97	3.5
Dec-2016	1,294	540	98	4.2
Jan-2017	852	449	99	3.5
Feb-2017	777	437	97	2.8
Mar-2017	1,149	512	98	3.8
Apr-2017	962	488	98	3.4
May-2017	1,316	508	98	9.5
Jun-2017	1,059	517	96	3.3
Jul-2017	1,100	498	97	8.1
Aug-2017	1,019	472	98	3.7
Sep-2017	1,052	474	98	6.4
Oct-2017	964	463	97	3.4
Nov-2017	1,103	507	97	4.5
Dec-2017	1,355	549	97	6.8
Jan-2018	1,069	508	98	3.7
Feb-2018	635	378	95	2.6
Mar-2018	1,097	510	98	4.0
Apr-2018	903	473	98	3.9
May-2018	1,051	504	96	3.7
Jun-2018	962	469	98	3.2
Jul-2018	1,038	494	97	4.6
Aug-2018	958	479	97	3.4
Sep-2018	794	431	95	2.9
Oct-2018	1,007	495	98	3.6
Nov-2018	880	466	99	2.9
Dec-2018	1,049	521	97	3.0
Jan-2019	995	489	96	3.3
Feb-2019	745	394	94	8.2
Mar-2019	1,064	507	96	3.3
Apr-2019	1,061	501	98	3.3

May-2019	1,149	532	97	3.4
Jun-2019	1,044	497	99	3.5
Jul-2019	1,138	515	97	4.0
Aug-2019	1,008	475	96	4.1
Sep-2019	922	488	97	2.8
Oct-2019	1,137	510	98	4.2
Nov-2019	1,283	502	98	13.0
Dec-2019	1,191	522	98	6.5
Jan-2020	751	401	96	7.6
Feb-2020	1,038	489	98	4.8
Mar-2020	1,128	535	97	3.6
Apr-2020	1,111	500	98	4.9
May-2020	1,110	499	98	4.6
Jun-2020	977	461	95	3.8
Jul-2020	866	415	95	4.1

Data Source: Ministry of the Interior, R.O.C (Taiwan)

Table A2. Complete results of triple difference regression models explaining the impact of flood and land subsidence on log farmland price (farm plot level analysis)

	(1) Month and village Fixed effects	(2) Month and Township Fixed effects
Flood (treatment)	-0.0718	-0.1344***
	(0.052)	(0.034)
After * Flood	0.0079	0.0301
	(0.079)	(0.046)
Land Subsidence (LS)	0.0251	-0.1424**
	(0.133)	(0.063)
LS * Flood	-0.0265	-0.0048
	(0.138)	(0.061)
LS * After	0.0224	0.0716
	(0.067)	(0.046)
LS * After * Flood	-0.0575	-0.1073**
	(0.091)	(0.053)
ln(Land size)	-0.1023***	-0.1235***
	(0.008)	(0.007)
Land Productivity	-0.0005	0.0060*
	(0.004)	(0.003)
Soil water retention index	0.0288	0.0535*
	(0.044)	(0.031)
ln(Agricultural Association)	-0.1896***	-0.2909***
	(0.052)	(0.022)
ln(Highway)	-0.0111	-0.0457***
	(0.024)	(0.015)
ln(Main road)	-0.1024***	-0.0847***
	(0.019)	(0.009)
ln(Taiwan High Speed Rail)	-0.0194	-0.0361*
	(0.044)	(0.020)
Constant	-2.6418***	-2.4768***
	(0.113)	(0.058)
Observations	55,129	55,129
R^2	0.84	0.62
F	19.39	62.88
p_value	0.00	0.00
Fixed Effect	Month*village	Month*Township
Cluster SE	village	village

The variable "After"does not appear on the table as it has been absorbed by month fixed effects.

Standard errors are in parentheses.

* $p < 0.10$, ** $p < 0.05$, and *** $p < 0.01$